Analyticity of partial wave scattering amplitudes and conformal mapping methods

1972 J. Phys. A: Gen. Phys. 5 981

(http://iopscience.iop.org/0022-3689/5/7/008)

J. Phys. A: Gen. Phys., Vol. 5, July 1972. Printed in Great Britain.

Analyticity of partial wave scattering amplitudes and conformal mapping methods†

A R CHOUDHARY and R B JONES

Physics Department, Queen Mary College, Mile End Road, London E1, UK

MS received 17 February 1972

Abstract. The problem of finding and calculating numerically a conformal mapping which simultaneously uniformizes several branchpoints in energy of a partial wave scattering amplitude is studied. Arguing from a potential scattering model, a general prescription is given for the construction of such conformal mappings in terms of automorphic forms. The automorphic forms are defined with respect to a group each of whose generators arises from one of the cuts in the energy plane of the scattering amplitude. The automorphic forms are calculated numerically from their Fourier series. The method is illustrated in detail for a relativistic single particle exchange model. Finally it is shown how the conformal mapping leads to simple representations of the analytic properties of the amplitude in terms of the uniformizing variable.

1. Introduction

Our aim is to discuss the problem of constructing and evaluating numerically uniformizing mappings for certain simple Riemann surfaces. The surfaces in question arise directly from model partial wave amplitudes, however the mappings we will construct could be of use also in some problems of two dimensional electrostatics or hydrodynamics. The mathematical technique we will use is the theory of automorphic forms in one variable. An introduction to the classical aspects of this theory may be found in the books by Fricke and Klein (1897, 1912) and by Ford (1951). A more modern and very lucid survey of the subject is the book 'Discontinuous Groups and Automorphic Functions' by Lehner (1964). Lehner's work includes many more recent results which were essential for our purposes. We will adhere as closely as possible to Lehner's notation below and we refer the reader for detailed definitions and proofs of theorems to his book. Although it is nothing new that uniformizing mappings involve automorphic functions (Ford 1951) we are not aware of any detailed description of how to use the relevant theorems for a numerical evaluation of such mappings. In this paper we hope to elucidate some of these more mundane considerations. In the next section we will introduce two simple models to illustrate how our mappings arise in particle physics. In § 3 we outline a general mathematical procedure. In §§ 4 and 5 we consider, for one of our models, the construction of certain automorphic forms by the Fourier expansion of Poincare series. In § 6 we discuss numerical evaluation of these functions and in § 7 we return to our model amplitude and possible analytic representations of it through the uniformizing variable.

† This work has been based in part on a PhD Thesis submitted to the University of London, 1971.

2. Two model amplitudes

An important aim of conformal mapping techniques in particle physics is to find a variable in terms of which a scattering amplitude may be easily approximated by rational functions (see eg Frazer 1961, or Cutkosky and Deo 1968; for other applications of conformal mapping in establishing upper bounds to scattering amplitudes see Baluny 1969). The conformal mapping used may be one confined to the physical sheet of the amplitude (Frazer 1961, Cutkosky and Deo 1968) or, if enough is known or assumed about the branchpoint structure, it may be a multisheet mapping which simultaneously uniformizes several branchpoints. Thus the effective range formula in potential scattering gives a rational approximation in terms of the variable $k = \sqrt{E}$, a two-sheeted uniformizing variable for the elastic threshold branchpoint in the partial wave amplitudes. Simple mathematical models of pion–pion partial wave amplitudes have been constructed in terms of a variable uniformizing the elastic threshold arising from the $\sqrt{\{(s-4)/s\}}$ phase space factor (Wanders and Piguet 1968). More recently potential theory models with a single logarithmic left hand branchpoint have been studied in terms of a uniformizing variable given by the elliptic modular function (Jones 1970, Choudhary and Jones 1970, Choudhary 1971). In these latter models the uniformizing variable opened the way to simple accurate approximations which have applications to the low energy nucleon–nucleon amplitudes (Choudhary 1971). In all these instances the uniformizing variable could be obtained from classical functions which offer no problem of numerical evaluation. Any generalization of these models, however, at once leads us to unknown mappings for which there is no standard method of evaluation.

Thus the potential theory model mentioned above (Jones 1970) concerns a partial wave amplitude $A(E)$ with a cut energy plane as in figure 1. The discontinuities across the cuts are of the form

$$\begin{aligned} &\text{disc } A(E) = 2i\sqrt{E}\,|A(E)|^2 \qquad 0 \leqslant E \leqslant +\infty \\ &\text{disc } A(E) = 2i\rho(E) \qquad -\infty \leqslant E \leqslant -\tfrac{1}{4}m^2 \end{aligned} \tag{1}$$

where $\rho(E)$ is assumed to be a rational function of $\sqrt{E}$. By analytic continuation (Jones 1970) one identifies the Riemann surface of $A(E)$ with the universal covering surface of

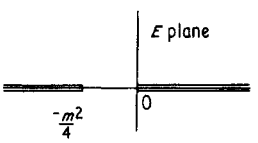

Figure 1. Cut E plane for the potential scattering model.

a thrice-punctured sphere and hence the amplitude is uniformized by the elliptic modular function $\lambda(\omega)$

$$E = k^2 = -m^2(\lambda(\omega)-\tfrac{1}{2})^2. \tag{2}$$

For this particular model the procedure may also be viewed as first uniformizing the unitarity branchpoint by the use of k and then independently uniformizing the left hand branchpoints in k (figure 2) by

$$k = im(\lambda(\omega)-\tfrac{1}{2}). \tag{3}$$

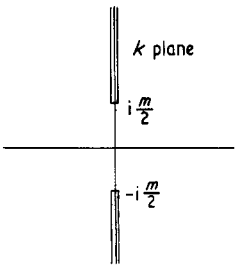

Figure 2. Cut k plane for the potential scattering model.

It is useful to summarize those features of $\lambda(\omega)$ which point the way to more general mappings. First, $\lambda(\omega)$ is a univalent automorphic function on the group $\Gamma(2)$, a subgroup of the modular group $\Gamma(1)$ (Ford 1951, Lehner 1964). $\Gamma(2)$ is a group of linear fractional transformations preserving an upper half ω plane H and represented in the usual way by real two-by-two unimodular matrices. $\Gamma(2)$ is generated by two transformations

$$S = \begin{pmatrix} 1 & 2 \\ 0 & 1 \end{pmatrix} \qquad V_1 = \begin{pmatrix} 1 & 0 \\ -2 & 1 \end{pmatrix} \tag{4}$$

and it has a fundamental region in H as shown in figure 3. Each generator of $\Gamma(2)$

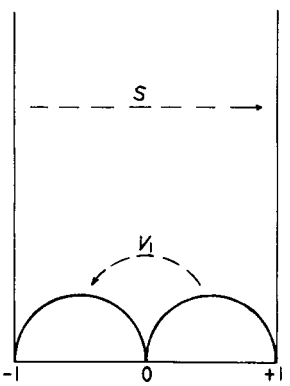

Figure 3. Fundamental region of $\Gamma(2)$ in the upper half ω plane H.

conjugates a pair of sides of the fundamental region in figure 3 where each such pair of sides corresponds to the two opposite sides of a cut in the k plane (figure 2). Each branchpoint in k is of infinite order and the associated transformations S and V_1 are parabolic transformations whose fixed points correspond to the finite branchpoints in k. The fundamental region is symmetric about the imaginary axis of ω, corresponding to the real analyticity of $A(E)$. Finally we note that $\lambda(\omega)$ can be expressed, using θ function identities, as

$$\lambda(\omega) = \left(\frac{\theta_2(\omega)}{\theta_3(\omega)}\right)^4 = -\frac{\theta_4^8(\omega)+\theta_2^8(\omega)-\theta_3^8(\omega)}{\theta_4^8(\omega)-\theta_2^8(\omega)+\theta_3^8(\omega)} \tag{5}$$

where $(\theta_4^8(\omega)+\theta_2^8(\omega)-\theta_3^8(\omega))$ and $(\theta_4^8(\omega)-\theta_2^8(\omega)+\theta_3^8(\omega))$ are respectively automorphic forms of dimension -4 on $\Gamma(2)$, in fact, Eisenstein series on $\Gamma(2)$.

Instead of uniformizing in two steps, it is equally instructive to view the procedure as a one step uniformization directly from E to ω. In terms of E the Riemann surface of $A(E)$ is a branched, not regular, covering surface of a punctured E sphere. The function $(\lambda(\omega)-\frac{1}{2})^2$ is a univalent automorphic function on the group Γ_3, also a subgroup of the modular group (Lehner 1964). Γ_3 is generated by S of equation (4) and the transformation

$$W_1 = \begin{pmatrix} 0 & -1 \\ 1 & 0 \end{pmatrix}. \tag{6}$$

A fundamental region for Γ_3 is shown in figure 4. We observe that the generator W_1, an elliptic transformation of order two, corresponds to the square root branching of order one at $E = 0$ in $A(E)$. The fixed point $\omega = \mathrm{i}$ of W_1 is an elliptic vertex corresponding to $E = 0$. Again each generator conjugates a pair of sides of the fundamental region corresponding to the opposite sides of a cut in the E plane.

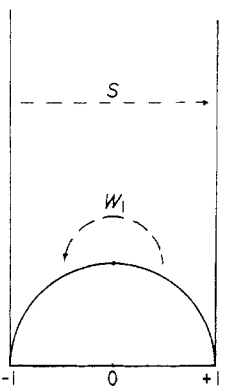

Figure 4. Fundamental region of Γ_3 in the upper half ω plane H.

The example above suggests a clear procedure to follow in a more general case with N branchpoints. However, it does not illustrate the difficulties that will also occur in a more general situation. Therefore, let us examine a slight generalization of the model above which at once illustrates such difficulties and the procedures for overcoming them. Consider a pion–pion partial wave amplitude with elastic unitarity only and a left hand cut due to single particle exchange. The amplitude $T(s)$ will be analytic in a cut s plane (pion mass set equal to one) as in figure 5. Across the cuts the discontinuities will be

$$\begin{aligned} \text{disc } T(s) &= 2\mathrm{i}\left(\frac{s-4}{s}\right)^{1/2} |T(s)|^2 \qquad 4 \leqslant s \leqslant +\infty \\ \text{disc } T(s) &= 2\mathrm{i}\rho(s) \qquad -\infty \leqslant s \leqslant 4-m_e^2 < 0 \end{aligned} \tag{7}$$

where $\rho(s)$ is a rational function of s and m_e is the mass of the exchanged particle. (We assume $m_e > 2$ for the purposes of illustration, $m_e \leqslant 2$ would be handled by an obvious modification below.) This model superficially resembles the potential theory model above in that there are three branchpoints in the physical sheet, one of order one at $s = 4$ and two of infinite order at $s = 4-m_e^2$ and $s = -\infty$. However, due to the phase

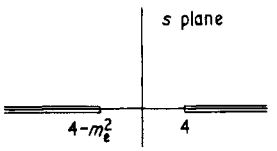

Figure 5. Cut s plane of the relativistic single particle exchange model.

space factor $\sqrt{\{(s-4)/s\}}$ in equation (7), $T(s)$ also has a branchpoint of order one at $s = 0$ on all unphysical sheets reached by continuation through the unitarity cut. Thus the typical sheet of the Riemann surface of $T(s)$ has four branchpoints, two of order one and two of infinite order.

This situation, with the unphysical sheets being more complicated than the physical sheet, is the first difficulty that is likely to occur in a more general problem with N branchpoints. In this model one cannot avoid the difficulty by uniformizing in two steps, first unwinding the unitarity branchpoints as in the first model above and then handling the left hand branchpoints separately. Such an attempt leads one to the problem of constructing automorphic forms on a group with an infinite number of generators, a problem outside the scope of the theorems we have available. Nor can one simply ignore the $s = 0$ branchpoints which for $m_e > 2$ are 'closer' to the low energy region above threshold than the branchpoint at $4-m_e^2$. The way around this difficulty is to put the $s = 0$ branchpoint into all the sheets and then to remove it later. In other words, instead of the actual Riemann surface $\mathscr{R}$ of $T(s)$, we consider $\hat{\mathscr{R}}$ a branched covering surface of $\mathscr{R}$. $\hat{\mathscr{R}}$ is to have all its sheets alike, with two branchpoints of order one and two of infinite order on each sheet. Later we shall see that $T(s)$ can be regarded as a function on $\hat{\mathscr{R}}$ subject to simple analytic constraint equations. Thus in a general situation one may have to work with some branched covering surface of the actual surface of interest. In our model this will be $\hat{\mathscr{R}}$ whose typical sheet is illustrated in figure 6 where we have numbered the sides of the cuts for later reference.

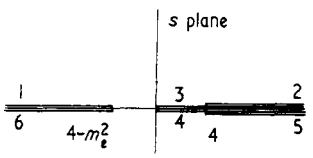

Figure 6. Typical sheet of the covering surface arising in the single particle exchange model.

A second difficulty concerns the parameter m_e which specifies where the left hand branchpoint is situated relative to the other three branchpoints. This parameter has a new significance it did not possess in the potential theory model above. Namely, m_e parametrizes a continuous family of conformally inequivalent surfaces, it is a modulus of $\hat{\mathscr{R}}$ (Lehner 1964, Springer 1957). Two surfaces $\hat{\mathscr{R}}$ for different m_e values cannot be conformally mapped on one another. Thus the uniformizing mapping for $\hat{\mathscr{R}}$ will depend on a parameter, and we shall see that it depends markedly on this parameter. In a general problem of this type with N branchpoints one would expect $N-3$ such parameters. This circumstance can noticeably complicate the numerical work required to evaluate the mapping function.

3. Some theorems of interest

The two models above suggest a general procedure for uniformization and also illustrate some difficulties that may arise. We now wish to state a general prescription for obtaining the mapping function and to illustrate it by numerical calculations in the relativistic model above. Thus we assume that we have a Riemann surface over an s plane with N branchpoints (including one at infinity) occurring in each sheet at points $s_1, s_2, s_{N-1}, \infty$. (To achieve this may already require going to a covering surface of the one of interest, as above.) We assume further that branchpoints of infinite order are present. Figure 7 illustrates what we have in mind and there we assume that the nearest left hand branchpoint s_{p+1} is of infinite order. Finally, we must know the order of each branchpoint to make the problem well defined.

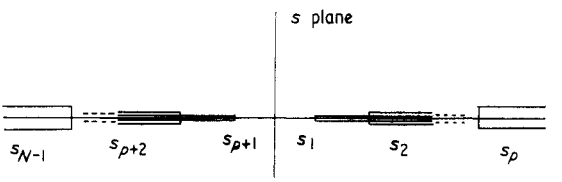

Figure 7. General configuration of N branchpoints in the s plane to be uniformized.

The general procedure to be followed is this. First construct a noneuclidean polygon R_0 in the upper half ω plane H (ie a polygon bounded by straight lines and arcs of circles, Lehner 1964) such that to each branchpoint there corresponds a cycle of vertices and to each piece of cut connecting adjacent branchpoints there corresponds a pair of sides of the polygon. To a branchpoint of infinite order there must correspond a cycle of parabolic vertices while to an algebraic branchpoint of order $k-1$ there must correspond a cycle of elliptic vertices of order k. Thus R_0 must have $2N-2$ sides and N distinct cycles of vertices. One parabolic vertex should be placed at $\omega = i\infty$; for the case illustrated in figure 7, this will correspond to s_{p+1}. Finally, construct R_0 to be symmetric about the imaginary axis of ω. This symmetry requirement will lead to nice reality properties of the mapping function and expresses the reflection symmetry in the real axis of the cut s plane of figure 7.

Next identify each pair of sides of R_0 corresponding to a piece of cut as conjugate sides under a linear fractional transformation. Form the group Γ generated by the $N-1$ such transformations associated with each pair of sides of R_0. By a basic theorem of Poincare, Γ is a group discontinuous in the upper half ω plane H with polygon R_0 as a fundamental region (Lehner 1964). The group has translations in it because we have assumed that there are branchpoints of infinite order present. Now use generalized Poincare series to compute everywhere regular automorphic forms of negative dimension on Γ and take the root of a suitable ratio of such forms to obtain a univalent automorphic function on Γ. This function $\Omega(\omega)$ will map H one-to-one and conformally onto the Riemann surface of interest regarded as a covering of the s plane, $s = \Omega(\omega)$.

Let us apply this prescription to our relativistic model with covering surface $\mathscr{R}$ whose cuts in s are illustrated in figure 6. Since there are two branchpoints of order one and two of infinite order we require a six sided polygon containing two parabolic cycles of vertices and two elliptic cycles of order two. Following the rules stated above we construct the polygon R_0 of figure 8. The sides of R_0 are numbered to correspond

to the sides of the cuts in figure 6. The branchpoint at $s = 4-m_e^2$ is represented by a cycle consisting of a single vertex at i∞. The $s = 0$ branchpoint of order one is represented by a cycle consisting of a single elliptic vertex at $\omega = \alpha$. The $s = 4$ branchpoint is represented by two vertices at $\omega = \beta$ and $\omega = -\bar{\beta}$ which together form an elliptic cycle of order two. Finally the parabolic vertices at $\omega = \pm 1$ form a cycle corresponding to $s = \infty$. Sides 3 and 4 meet at an angle of π at $\omega = \alpha$ while sides 2 and 3, and sides 4 and 5 meet at an angle of $\pi/2$ to form the appropriate elliptic cycles.

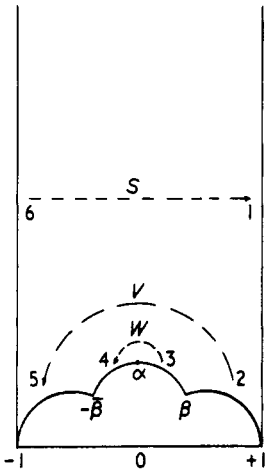

Figure 8. Fundamental region of Γ in the upper half ω plane H. Here $\alpha = i/\rho$ and $\beta = (\gamma - 1 + i/\rho)/\gamma$.

Sides 1 and 6, 1 and 2, 5 and 6 are tangent where they meet to form parabolic vertices. We are free to choose the width of R_0 to be two by a simple dilatation. Fixing the width and requiring symmetry about the imaginary axis leaves one free real parameter which we have denoted ρ. It represents the geometric freedom of choosing the intersection point β of sides 2 and 3. The parameter ρ is analogous to m_e, it is the modulus of $\hat{\mathscr{R}}$ as represented by the half plane H.

It is easy to see that the three transformations which conjugate the pairs of sides of R_0 corresponding to each cut in s are

$$S = \begin{pmatrix} 1 & 2 \\ 0 & 1 \end{pmatrix}$$
$$W = \begin{pmatrix} 0 & -1/\rho \\ \rho & 0 \end{pmatrix} \qquad V = \begin{pmatrix} \gamma & 1-\gamma \\ -1-\gamma & \gamma \end{pmatrix} \tag{8a}$$

where

$$\gamma = \frac{\rho^2+1}{\rho^2-1} \qquad 1 < \rho < +\infty. \tag{8b}$$

These three transformations generate a group which we shall denote by Γ with fundamental region R_0 as in figure 8. The group Γ depends on the parameter ρ in a marked

way. Indeed, Γ reduces to each of the groups arising from the potential model in an appropriate limit, namely

$$\lim_{\rho \to 1} \Gamma = \Gamma_3$$
$$\lim_{\rho \to \infty} \Gamma = \Gamma(2). \tag{9}$$

These limits are geometrically obvious since the fundamental region R_0 of Γ reduces to the appropriate fundamental regions of Γ_3 and $\Gamma(2)$ (figures 4 and 3) in the respective limits. These limits will be of use later in checking the accuracy of numerical calculations.

Having shown how to construct Γ starting from a model in the s plane, we now consider the construction of automorphic forms and functions on Γ. Since we aim ultimately to find a univalent automorphic function on Γ, let us first verify that such a function exists. By a fundamental theorem a univalent function will exist if, and only if, the group is of genus zero (Lehner 1964). The genus g is determined from the fundamental region to be

$$g = \tfrac{1}{2}(n+1-c) \tag{10}$$

where c is the number of independent cycles of vertices, and n is the number of pairs of conjugate sides in the fundamental region (Lehner 1964). In our general case of N branchpoints mentioned above, $c = N$ and $n = N-1$, hence $g = 0$ in all cases and a univalent automorphic function will exist on the group.

To compute this function we want to express it, as in the case of the elliptic modular function in equation (5), in terms of a quotient of suitable automorphic forms. Recall that an automorphic form $F(\omega)$ of dimension $-r$, defined on a group Γ discontinuous in H, is a function $F(\omega)$ obeying the transformation law

$$F(M\omega) = v(M)(c\omega+d)^r F(\omega) \tag{11}$$

where $M = \left(\begin{smallmatrix} a & b \\ c & d \end{smallmatrix}\right)$ is an element of Γ, $M\omega = (a\omega+b)/(c\omega+d)$, and $v(M)$ is a multiplier system on Γ (Lehner 1964). $F(\omega)$ is required to be meromorphic in H with parabolic vertices included (Lehner 1964). In what follows we shall use only the trivial multiplier system $v(M) = 1$ for all M in Γ. In addition we shall use only forms of negative even integral dimension, that is, $r = 2m$ where m is a positive integer, and $m > 1$ to ensure convergence of Poincare series.

Fortunately there is a very complete theory of such forms. We will quote some of the results most useful for our present purpose. The first important result is that the collection of everywhere regular forms on Γ, of fixed dimension $-r$, forms a finite dimensional vector space (Lehner 1964) which we shall denote $C^+(\Gamma, -r)$, suppressing mention of the multiplier system which is trivial in our case. Here regular has a technical definition at vertices but its usual meaning elsewhere in H (Lehner 1964). A cusp form is an element of $C^+(\Gamma, -r)$ which vanishes at all cusps (parabolic vertices) in the fundamental region. The collection of cusp forms constitutes a linear subspace of $C^+(\Gamma, -r)$ which we denote by $C^0(\Gamma, -r)$. We denote the orthogonal complement of C^0 in C^+ by E

$$C^+ = E \oplus C^0. \tag{12}$$

Of basic importance is the fact that the dimensions of these vector spaces are determined

by $-r$ and the geometry of the fundamental region. When the multiplier system is trivial ($v(M) = 1$) the results are (Lehner 1964)

$$\dim E = \sigma_0 \tag{13}$$

where σ_0 is the number of inequivalent parabolic cusps in R_0, and

$$\dim C^+(\Gamma, -2m) = (2m-1)(g-1) + \sum_i [m(1-1/l_i)] \tag{14}$$

where g is the genus of the group, the sum goes over all cycles in the fundamental region, l_i is the order of the ith cycle ($l_i = \infty$ for parabolic cycles) and $[k]$ denotes the greatest integer less than or equal to k. In our case there are two parabolic cycles in R_0, hence

$$\dim E = 2 \tag{15}$$

while (14) gives

$$\dim C^+(\Gamma, -2m) = 1 + 2[m/2]. \tag{16}$$

From (12) we have

$$\dim C^0(\Gamma, -2m) = 2[m/2] - 1. \tag{17}$$

Thus E is a two dimensional vector space while the space of cusp forms increases in size as the dimension $-2m$ of the cusp forms increases in magnitude.

The relations above tell how many independent forms can exist on Γ. It is important also to know about the zeros of these forms as functions of ω. In general, if one considers the sum of the orders of a form in its fundamental region (ie the number of zeros minus the number of poles), this number J is determined by the dimension $-2m$ of the form and by the structure of the fundamental region. One may show that

$$J = m\left(n - 1 - \sum_i 1/l_i\right) \tag{18}$$

where n is the number of pairs of sides of R_0, the sum is over cycles of R_0 and l_i is the order of the ith cycle. (Note that the order of a form at an elliptic vertex is not necessarily an integer (Lehner 1964).) Since we are considering only regular forms, J just gives the total number of zeros of the form in R_0. In our case (18) becomes

$$J = m. \tag{19}$$

Thus, as m increases, the size of the space C^+, as well as the number of zeros of its elements, increases. Note that for an automorphic function ($m = 0$), (18) gives $J = 0$, that is, an automorphic function takes each complex value the same number of times in the fundamental region. This number is called its valence. If we form an automorphic function as the quotient of forms in $C^+(\Gamma, -2m)$, we have that the valence of such a function will be m. In what follows we will choose $m = 2$ since the Poincare series do not converge for $m = 1$. We will construct forms of dimension -4 and by taking their quotient obtain a divalent automorphic function on Γ. By suitably choosing the forms we can arrange for this divalent function to have its two zeros coincident and its two poles coincident. Then by simply taking the square root we get the desired univalent mapping function.

4. Poincare series

Having described the group Γ and the forms that exist on it, we now wish to construct these forms in a way amenable to numerical calculation. For this we use the Poincare series. Let us first establish some notation (Lehner 1964). Our region R_0 has two inequivalent parabolic cusps. One is at $\omega = i\infty$ and the other we may take to be the cusp at $\omega = +1$. Let us denote these by $p_0 = i\infty$, $p_1 = +1$. The point p_0 is a fixed point of the transformation $P_0 = S$ while p_1 is a fixed point of $P_1 = V^{-1}S^{-1}$. Define transformations (Lehner 1964)

$$A_0 = \begin{pmatrix} 1 & 0 \\ 0 & 1 \end{pmatrix} \qquad A_1 = \begin{pmatrix} 0 & -1 \\ 1 & -1 \end{pmatrix} \tag{20}$$

with the property

$$A_j p_j = i\infty \qquad j = 1, 2. \tag{21}$$

Further, $A_j P_j A_j^{-1}$ is a parabolic transformation fixing $i\infty$. Hence define

$$U^{\lambda_j} = \begin{pmatrix} 1 & \lambda_j \\ 0 & 1 \end{pmatrix} = A_j P_j A_j^{-1} \qquad j = 1, 2 \tag{22}$$

where

$$\lambda_0 = 2 \qquad \lambda_1 = \gamma + 1. \tag{23}$$

The transformation U^{λ_j} generates a subgroup Γ_∞^j of $A_j \Gamma A_j^{-1}$, Γ_∞^j is a group of parabolic transformations fixing the point at infinity. Remembering that our multiplier system is the trivial one ($v(M) = 1$) the generalized Poincare series (Lehner 1964) are defined by

$$G_{-2m}(\omega, 1, A_j, \Gamma, v) = \sum_{L \in (S)} (c\omega + d)^{-2m} \exp\left(\frac{2\pi i v}{\lambda_j}(L\omega)\right). \tag{24}$$

In this expression v is an integer, (S) denotes a system of right cosets of $A_j\Gamma$ with respect to Γ_∞^j

$$(S) = \Gamma_\infty^j \backslash A_j \Gamma$$

$L = \left(\begin{smallmatrix} a & b \\ c & d \end{smallmatrix}\right)$ is a representative of a coset in $A_j\Gamma$ and the sum runs over all cosets, that is, we sum over all matrices L in $A_j\Gamma$ with distinct second row matrix elements c and d. The series in (24) converges absolutely and uniformly on compact subsets of the open upper half ω plane and obeys the transformation law (11) (Lehner 1964).

For $v > 0$, $G_{-2m}(\omega, 1, A_j, \Gamma, v)$ vanishes at all parabolic cusps in R_0, that is, it is a cusp form belonging to $C^0(\Gamma, -2m)$ (Lehner 1964). These Poincare series span the space of cusp forms. Since $v = 1, 2, 3, \ldots$ there are infinitely many such series while $C^0(\Gamma, -2m)$ is only of finite dimension. Thus linear relations exist among the series for different values of v, and, for certain v values, the series may vanish identically (Lehner 1964). The series for $v = 0$ are called Eisenstein series and have the distinctive property that

$$E(\omega, A_j) = G_{-2m}(\omega, 1, A_j, \Gamma, 0)$$

takes the value two at the cusp p_j and vanishes at all other inequivalent cusps. These series span the space E mentioned above.

In our model we are working with $m = 2$. From equations (15), (16) and (17) we see that $\dim C^+ = 3$, $\dim E = 2$, $\dim C^0 = 1$. Thus $C^+(\Gamma, -4)$ is spanned by the two Eisenstein series $E(\omega, A_0)$ and $E(\omega, A_1)$ together with one cusp form which we will take to be

$$G(\omega, 1) = G_{-4}(\omega, 1, A_0, \Gamma, 1). \tag{25}$$

From equation (19) the sum of the orders of these forms is two. Since $G(\omega, 1)$ is a cusp form which must vanish at both p_0 and p_1, these are its only zeros and they are simple zeros. $E(\omega, A_0)$ and $E(\omega, A_1)$ each vanish at one parabolic cusp but not at the other. Numerical calculation shows that $E(\omega, A_j)$ has a simple zero at p_j and a second zero lying on sides 2 or 3 of R_0. This second zero moves as a function of the modulus ρ. Because these moving zeros of $E(\omega, A_0)$ and $E(\omega, A_1)$ are not coincident, we cannot as in equation (6) directly get a univalent function as a quotient of Eisenstein series on Γ. Instead, we must utilize the cusp form as well in order to form linear combinations $E(\omega, A_j) + a_j G(\omega, 1)$ which have double zeros rather than a pair of simple zeros.

5. Fourier expansions

The Poincare series in (24) defining $G_{-2m}(\omega, 1, A_j, \Gamma, v)$ is of little help in studying the zeros of these forms nor is it particularly useful for numerical evaluation. In fact, it is possible to carry out an explicit partial summation of (24) to get a Fourier expansion of the $G_{-2m}(\omega, 1, A_j, \Gamma, v)$ about any of the parabolic cusps of the fundamental region (Lehner 1964). Below we will quote these general results of Lehner (1964) in the concrete form applicable to our special case. Thus the Eisenstein series $E(\omega, A_j)$ have expansions about $p_0 = i\infty$

$$E(\omega, A_0) = 2 + \sum_{q=1}^{\infty} c_q(A_0, 0) \exp\left(\frac{i2\pi q\omega}{\lambda_0}\right) \tag{26a}$$

$$E(\omega, A_1) = \sum_{q=1}^{\infty} c_q(A_1, 0) \exp\left(\frac{i2\pi q\omega}{\lambda_0}\right) \tag{26b}$$

while the cusp form $G(\omega, 1)$ has an expansion

$$G(\omega, 1) = 2\exp\left(\frac{i2\pi\omega}{\lambda_0}\right) + \sum_{q=1}^{\infty} c_q(A_0, 1) \exp\left(\frac{i2\pi q\omega}{\lambda_0}\right). \tag{26c}$$

Numerical evaluation of $c_1(A_1, 0)$ (see below) shows it to be nonzero and hence $E(\omega, A_1)$ has a zero of order one at $i\infty$. However, the linear combination

$$E(\omega, A_1) - \left(\frac{c_1(A_1, 0)}{2 + c_1(A_0, 1)}\right) G(\omega, 1)$$

is a regular form of dimension -4 with a double zero at $i\infty$.

To obtain a form with a double zero at the finite cusp $p_1 = +1$ we require the Fourier expansions of $E(\omega, A_0)$ and $G(\omega, 1)$ about the finite cusp p_1 (Lehner 1964).

These take the form

$$(\omega-1)^4 E(\omega, A_0) = \sum_{q=1}^{\infty} a_q \exp\left(\frac{i2\pi q}{\lambda_1}(A_1\omega)\right) \tag{27a}$$

$$(\omega-1)^4 G(\omega, 1) = \sum_{q=1}^{\infty} b_q \exp\left(\frac{i2\pi q}{\lambda_1}(A_1\omega)\right). \tag{27b}$$

To get the coefficients a_q and b_q in terms of Lehner's coefficients we must use the A_1 transforms of $E(\omega, A_0)$ and $G(\omega, 1)$. If L is a fixed linear fractional transformation, the L transform of a form $F(\omega)$ of dimension $-r$ is defined by (Lehner 1964)

$$\begin{aligned} F(\omega)|_L &= (g\omega+h)^{-r} F(L^{-1}\omega) \\ L^{-1} &= \begin{pmatrix} \cdot & \cdot \\ g & h \end{pmatrix}. \end{aligned} \tag{28}$$

If $F(\omega)$ is an automorphic form on group Γ, $F(\omega)|_L$ is an automorphic form on the group $L\Gamma L^{-1}$. Denote by Γ' the group $A_1\Gamma A_1^{-1}$. Thus

$$E(\omega, A_0)|_{A_1} = (-\omega)^{-4} E(A_1^{-1}\omega, A_0). \tag{29}$$

However, as Lehner (1964) shows

$$E(\omega, A_0)|_{A_1} = G_{-4}(\omega, 1, A_0, \Gamma, 0)|_{A_1} = G_{-4}(\omega, 1, A_1^{-1}, \Gamma', 0). \tag{30}$$

Thus from (30), $E(\omega, A_0)|_{A_1}$ is an Eisenstein series on Γ'. Hence as a generalized Poincare series on Γ' it has an expansion at $i\infty$ of the form

$$G_{-4}(\omega, 1, A_1^{-1}, \Gamma', 0) = \sum_{q=1}^{\infty} c'_q(A_1^{-1}, 0) \exp\left(\frac{i2\pi q\omega}{\lambda_1}\right). \tag{31}$$

Replacing ω by $A_1\omega$ in (31) and using (29) and (30) gives

$$(\omega-1)^4 E(\omega, A_0) = \sum_{q=1}^{\infty} c'_q(A_1^{-1}, 0) \exp\left(\frac{i2\pi q}{\lambda_1}(A_1\omega)\right) \tag{32}$$

and the coefficient a_q is given by

$$a_q = c'_q(A_1^{-1}, 0). \tag{33}$$

A similar argument for $G(\omega, 1)$ gives

$$b_q = c'_q(A_1^{-1}, 1). \tag{34}$$

Thus the linear combination

$$E(\omega, A_0) - \frac{c'_1(A_1^{-1}, 0)}{c'_1(A_1^{-1}, 1)} G(\omega, 1)$$

is an everywhere regular form of dimension -4 with a double zero at $p_1 = +1$. If

we form the function

$$\tilde{\Omega}(\omega) = \left\{ \left(E(\omega, A_1) - \frac{c_1(A_1, 0)}{2 + c_1(A_0, 1)} G(\omega, 1) \right) \left(E(\omega, A_0) - \frac{c_1'(A_1^{-1}, 0)}{c_1'(A_1^{-1}, 1)} G(\omega, 1) \right)^{-1} \right\}^{1/2} \tag{35}$$

we obtain a univalent automorphic function on Γ.

Finally we must specify how to express the various Fourier coefficients above in terms of information about the group Γ. First consider the coefficients $c_q(A_0, 0)$ in the expansion (26*a*) of $E(\omega, A_0)$. Lehner's general expression gives

$$c_q(A_0, 0) = \left(\frac{2\pi}{\lambda_0} \right)^4 \frac{q^3}{3} \sum_c \frac{1}{c^4} \sum_d \exp\left(\frac{i2\pi qd}{\lambda_0 c} \right) \tag{36a}$$

where c and d are elements of a transformation $M = \left(\begin{smallmatrix} a & b \\ c & d \end{smallmatrix}\right)$ in Γ and the summation runs over a restricted class of matrices in Γ uniquely specified by the conditions

$$c > 0 \qquad 0 \leqslant -d < \lambda_0 c \qquad 0 \leqslant a < \lambda_0 c. \tag{36b}$$

This sum and the condition (36*b*) can be simplified using the fact demonstrated in the appendix that if $\left(\begin{smallmatrix} a & b \\ c & d \end{smallmatrix}\right)$ belongs to the collection of matrices $A_j\Gamma$, then $\left(\begin{smallmatrix} a & -b \\ -c & d \end{smallmatrix}\right)$ also belongs to $A_j\Gamma$. Also, the only matrix with $d = 0$ or $a = 0$ contributing to (36*a*) is W. Thus (36*a*) becomes

$$c_q(A_0, 0) = \left(\frac{2\pi}{\lambda_0} \right)^4 \frac{q^3}{3} \left\{ \frac{1}{\rho^4} + \sum_c \frac{2}{c^4} \sum_d \cos\left(\frac{2\pi qd}{\lambda_0 c} \right) \right\} \tag{37a}$$

with matrices in the summation restricted by

$$c > 0 \qquad 0 < -d < \tfrac{1}{2} c\lambda_0 \qquad 0 < a < c\lambda_0. \tag{37b}$$

For the cusp form $G(\omega, 1)$ the expansion (26*c*) requires

$$c_q(A_0, 1) = \left(\frac{4\pi}{\lambda_0} \right) (q)^{3/2} \sum_c \frac{1}{c} J_3\left(\frac{4\pi}{c\lambda_0} \sqrt{q} \right) \sum_d \exp\left(\frac{i2\pi}{\lambda_0 c} (a + qd) \right) \tag{38}$$

where J_3 is a Bessel function of order three and the matrix elements a, c, and d are again restricted by (36*b*). A similar simplification gives

$$c_q(A_0, 1) = \frac{4\pi}{\lambda_0} (q)^{3/2} \left\{ \frac{1}{\rho} J_3\left(\frac{4\pi}{\rho\lambda_0} \sqrt{q} \right) + \sum_c \frac{2}{c} J_3\left(\frac{4\pi}{c\lambda_0} \sqrt{q} \right) \sum_d \cos\left(\frac{2\pi}{\lambda_0 c} (a + qd) \right) \right\} \tag{39}$$

where a, c, and d satisfy (37*b*). For the coefficient $c_q(A_1, 0)$ arising from $E(\omega, A_1)$, the sum is formally the same as (36) but over matrices $\left(\begin{smallmatrix} a & b \\ c & d \end{smallmatrix}\right)$ in $A_1\Gamma$ obeying $c > 0$, $0 \leqslant -d < \lambda_0 c$, and $0 \leqslant a < \lambda_1 c$. There is no matrix in $A_1\Gamma$ with $d = 0$, and the only matrix contributing with $a = 0$ is A_1. On simplifying we get

$$c_q(A_1, 0) = \left(\frac{2\pi}{\lambda_0} \right)^4 \frac{q^3}{3} \left\{ \exp\left(\frac{-i2\pi q}{\lambda_0} \right) + \sum_c \frac{2}{c^4} \sum_d \cos\left(\frac{2\pi qd}{\lambda_0 c} \right) \right\} \tag{40a}$$

with c and d restricted by

$$c > 0 \qquad 0 < -d < \tfrac{1}{2}c\lambda_0 \qquad 0 < a < c\lambda_1 . \tag{40b}$$

We require expressions for $c'_q(A_1^{-1}, 0)$ and $c'_q(A_1^{-1}, 1)$ associated with expansions about $p_1 = +1$. These coefficients are defined with respect to $\Gamma' = A_1 \Gamma A_1^{-1}$ exactly as the unprimed coefficients are defined with respect to Γ. Thus

$$c'_q(A_1^{-1}, 0) = \left(\frac{2\pi}{\lambda_1}\right)^4 \frac{q^3}{3}\left\{1 + \sum_{c'} \frac{2}{c'^4} \sum_{d'} \cos\left(\frac{2\pi q d'}{\lambda_1 c'}\right)\right\} \tag{41a}$$

with

$$c' > 0 \qquad 0 < -d' < c'\lambda_1 \qquad 0 < a' < \tfrac{1}{2}c'\lambda_0 \tag{41b}$$

and

$$c'_q(A_1^{-1}, 1) = \left(\frac{4\pi}{\lambda_1}\right)\left(\frac{\lambda_0 q}{\lambda_1}\right)^{3/2}\left[-J_3\left(4\pi\sqrt{\frac{q}{\lambda_0\lambda_1}}\right) + \sum_{c'} \frac{2}{c'} J_3\left(\frac{4\pi}{c'}\sqrt{\frac{q}{\lambda_0\lambda_1}}\right) \sum_{d'} \cos\left\{\frac{2\pi}{c'}\left(\frac{a'}{\lambda_0} + \frac{qd'}{\lambda_1}\right)\right\}\right] \tag{42}$$

where the first term in (41*a*) and (42) represents the matrix $-A_1^{-1}$. The summations in (41*a*) and (42) are over matrices $\left(\begin{smallmatrix} a' & b' \\ c' & d' \end{smallmatrix}\right)$ in $A_1^{-1}\Gamma'$ restricted by (41*b*). Since $A_1^{-1}\Gamma' = \Gamma A_1^{-1}$, this set of matrices is just the collection of negative inverses of matrices in $A_1\Gamma$. Thus equations (40*a*), (41*a*) and (42) involve basically only one matrix tabulation rather than two tabulations.

6. Numerical procedures

Sections 4 and 5 provide exact analytic expressions for the function $\tilde{\Omega}(\omega)$. To calculate $\tilde{\Omega}(\omega)$ numerically involves at least two problems. The first problem is to tabulate the restricted class of matrices that contribute to the sums above for the Fourier coefficients. The second problem is to estimate how accurately the sums are given by using only a finite set of matrices.

Our first task is to identify matrices which contribute to the sums in order of increasing c values. This is easy for the modular group where the c values are integers. In more general groups such as Γ we are aware of no way to predict the distribution of c values. An added complication is that every element of Γ depends on the modulus ρ, hence a given matrix may contribute significantly only over a narrow range as ρ varies from 1 to ∞. However, it is possible to give a rough algorithm for tabulating matrices based on the geometry of the half plane H. To explain this, consider the sums in equations (37*a*) and (39) involving matrices M in Γ obeying condition (37*b*). The action of such a transformation in H is $M(i\infty) = a/c$, $M(-d/c) = i\infty$. That is, the point $i\infty$ goes onto the real axis between 0 and 2 while the point $(-d/c)$ also on the real axis between 0 and 1 is sent to $i\infty$. Recall that under the action of Γ the fundamental region R_0 is transformed so that its copies R_n exactly partition the half plane H (Lehner 1964). The region between R_0 and the real axis is partitioned as shown in figure 9. Thus we may restate the observation above by saying that the desired transformation M (apart from trivial translations by powers of S) sends R_0 onto one of its copies with a vertex on the real axis between -1 and 1. Thus from a diagram such as figure 9 one can systematically

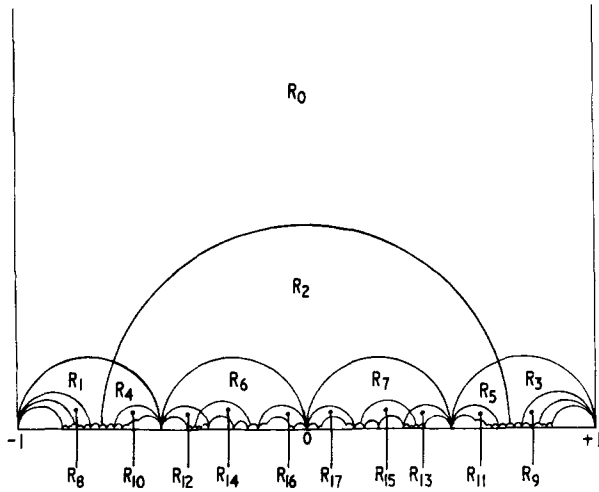

Figure 9. Partition of the upper half ω plane H by the action of Γ.

list transformations having this effect. In making such a list one gets the matrices in rough order of increasing c values. To see this, consider

$$\omega' = M\omega = \frac{a\omega+b}{c\omega+d}$$

where ω lies in R_0 and ω' lies in R_n obtained from R_0 by M. We see that

$$\left|\frac{d\omega'}{d\omega}\right|^2 = \frac{1}{c^4}\frac{1}{|\omega+(d/c)|^4}.$$

Taking into account (37*b*) we may say that $1/c^4$ is of the order of the ratio of the local element of euclidean area at ω' in R_n to the local element of euclidean area at ω in R_0. That is, $1/c^4$ is a rough measure of how euclidean area is diminished in going from R_0 to R_n by M. As is evident from figure 9, the euclidean area of R_n rapidly decreases near the real axis, hence the associated transformations have rapidly increasing values of c. With a bit of practice one may thus find all matrices with values of c lying in a fixed finite interval, $0 \leqslant c \leqslant c_0$.

A similar procedure gives matrices in $A_1\Gamma$. If M is a matrix in $A_1\Gamma$ obeying the conditions (40*b*), then M maps R_0 (apart from right translations by U^{λ_0} or left translations by U^{λ_1}) onto a polygon in the A_1 transform of H with a vertex on the real axis between 0 and λ_1. Thus one constructs the A_1 transform of figure 9 which is shown in figure 10 and again tabulates matrices using the area criterion. One must remember in doing this that both figures 9 and 10 vary considerably as ρ varies.

We have found those matrices satisfying conditions (37*b*), (40*b*), (41*b*) with c values obeying $0 \leqslant c \leqslant 6$ for at least some value of ρ in the range $1 < \rho < +\infty$. These are listed in table 1. Although many matrices are given there, at any one fixed value of ρ only a few will contribute significantly. Recall also that the contributions of W, A_1, and A_1^{-1} have been explicitly written in the summations of § 5.

By using only c values obeying $0 \leqslant c \leqslant 6$, how accurately will the Fourier coefficients of § 5 be given? We are aware of no sharp estimate for the remainder in such

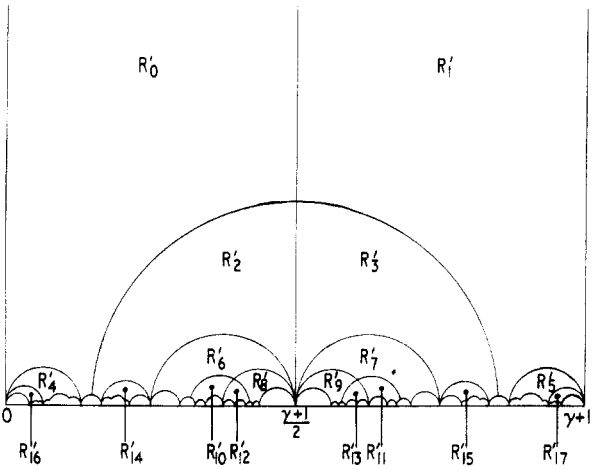

Figure 10. Partition of the upper half ω plane H by $\Gamma' = A_1 \Gamma A_1^{-1}$.

Table 1. In column 1 are listed leading matrices in Γ satisfying equation (37*b*). In column 2 are leading matrices in $A_1\Gamma$ satisfying equation (40*b*). The matrices in ΓA_1^{-1} satisfying equation (41*b*) are obtained as the negative inverses of the matrices in column 2

1	2
W	A_1
$-SV$	A_1V
$-SV^2$	A_1V^2
$-SV^3$	$A_1V^{-1}SV$
$(SV)^2$	$-A_1V^{-1}SW$
$-(SV)^3$	$-A_1V^{-1}S^2W$
$(SW)^2$	$-A_1V^{-1}(SW)^2$
$(SW)^3$	$-A_1WSW$
$(SW)^4$	$-A_1WS^2W$
$(SW)^5$	$-A_1W(SW)^2$
$(SW)^6$	$-A_1V^{-1}W$
SWS^2W	$-A_1V^{-1}WSW$
SWS^3W	$-A_1V^{-1}W(SW)^2$
$-WS^{-1}WSW$	$A_1WS^{-1}WV$
WV	$A_1WS^{-1}WSW$
WV^2	A_1WVSV
	$-A_1WVS^2W$
	$-A_1V^2W$

sums. However, we can apply two numerical tests which give a reasonable idea of the accuracy. The first test rests on the observation (9) that as $\rho \to 1$ and $\rho \to \infty$ Γ reduces respectively to Γ_3 and $\Gamma(2)$. Similarly the Eisenstein series $E(\omega, A_0)$ should reduce to the corresponding Eisenstein series for Γ_3 and $\Gamma(2)$. These are

$$2\theta_3^8(\omega) \quad \text{and} \quad \theta_4^8(\omega)+\theta_3^8(\omega)-\theta_2^8(\omega).$$

In table 2 we compare the exact limiting coefficients taken from the θ functions with numerical values computed from (37*a*) for $\rho = 1{\cdot}0001$ and $\rho = 50$. The comparison shows the numerical coefficients approaching the correct limits with an accuracy of

Table 2. Fourier coefficients $c_n(A_0, 0)$ for $E(\omega, A_0)$ in the $\Gamma(2)$ and Γ_3 limits

	$\rho = 50$	$\rho = \infty$ ($\Gamma(2)$ limit)	$\rho = 1{\cdot}0001$	$\rho = 1$ (Γ_3 limit)
c_1	−0·00	0·00	32·01	32·00
c_2	−32·03	−32·00	223·98	224·00
c_3	0·18	0·00	896·46	896·00
c_4	223·76	224·00	2272·31	2272·00
c_5	−1·30	0·00	4033·38	4032·00
c_6	−896·38	−896·00	6275·15	6272·00
c_7	7·02	0·00	10974·74	11008·00
c_8	2308·53	2272·00	18695·40	18656·00
c_9	−18·46	0·00	24215·57	24224·00

about one part in 10^3. The comparison suggests that the terms neglected contribute a remainder of the order of the last term $(1/6)^4$ included in the numerical summation. A second test is based on the obvious fact that error in the coefficients will appear in the Fourier series as error in evaluating the forms themselves. Now, as shown in the Appendix, we know the exact phase of the forms along the boundary of R_0. A comparison of the phases of our numerical evaluations with the exact phases along side 3 of R_0 is given in tables 3, 4 and 5 for $E(\omega, A_0)$, $E(\omega, A_1)$ and $G(\omega, 1)$. Again, the agreement is good for a range of ρ values and suggests that the Fourier coefficients are known accurately to about one part in 10^3.

Table 3. Phase relations for $E(\omega, A_0)$ $\omega = x + iy$, $y = (1/\rho)\sqrt{(1-\rho^2x^2)}$ (on side 3)

	Phases (rad)					
x	$\rho = 1{\cdot}2$		$\rho = \sqrt{2}$		$\rho = 2$	
	Approx	Exact	Approx	Exact	Approx	Exact
0·1	0·2406	0·2406	0·284	0·284	0·404	0·403
0·2	0·4847	0·4847	0·574	0·574	0·828	0·823
0·3	0·7366	0·7365	0·878	0·876	1·301	1·287
0·4	1·0014	1·0013	1·207	1·203		
0·5	1·2875	1·2870				

Table 4. Phase relations for $E(\omega, A_1)$ $\omega = x + iy$, $y = (1/\rho)\sqrt{(1-\rho^2x^2)}$ (on side 3)

	Phases (rad)					
x	$\rho = 1{\cdot}2$		$\rho = \sqrt{2}$		$\rho = 2$	
	Approx	Exact	Approx	Exact	Approx	Exact
0·1	0·2400	0·2406	0·285	0·284	0·404	0·403
0·2	0·4835	0·4847	0·575	0·574	0·842	0·823
0·3	0·7346	0·7365	0·879	0·876	1·272	1·287
0·4	0·9987	1·0013	1·209	1·203		
0·5	1·2835	1·2870				

Table 5. Phase relations for $G(\omega, 1)$ ($\rho = \sqrt{3}$) $\omega = x+iy$, $y = (1/\rho)\sqrt{(1-\rho^2x^2)}$ (on side 3)

	Phases (rad)	
x	Approx	Exact
0·05	0·173	0·173
0·10	0·347	0·348
0·15	0·524	0·526
0·20	0·706	0·708
0·30	1·090	1·093
0·40	1·527	1·531

The numerical results presented above show that automorphic forms can be computed numerically in a rather simple fashion using the Fourier expansions of such forms. In an application of the mapping function above one might of course desire increased numerical precision. The obvious way to achieve this is to include more matrices with larger c values in the sums above. We have already indicated how this can be done. However, an alternative procedure might be based on the observation that, for forms of dimension $-2m$, the sums for the Fourier coefficients go as c^{-2m}. Above we chose $m = 2$ in analogy with the potential theory model. However, by going to larger m values one could suppress even further the contributions from large c values. There is a penalty of course for trying this. Equations (17) and (19) tell us that both the number of independent cusp forms and the order J increase with m. As J increases, so does the valence of the function we obtain as a quotient of such forms. As a consequence, we must take larger linear combinations of the independent forms in order to make zeros coincide at $i\infty$ and $+1$. For m an even integer the number of independent cusp forms increases just rapidly enough to construct such linear combinations and then the mth root of the quotient gives a univalent function. The numerical problems that arise in such a procedure spring from the problem of finding a linearly independent set of Poincare series (24) to span $C^0(\Gamma, -2m)$. To find such a set would involve testing the rank of an $(m-1)$ by $(m-1)$ dimensional matrix of Fourier coefficients (Lehner 1964) at different ρ values. In the case $m = 2$ the matrix has only one element, but the ρ dependence is still important for that element vanishes for some ρ value between 7 and 8 implying the identical vanishing of $G(\omega, 1)$ at that value of ρ. As m increases the difficulty of finding an independent set of forms will correspondingly increase. Nevertheless, for m not too large, this second technique should be a useful method of improving the precision of numerical calculations.

Another important point concerning numerical calculation is that the forms above may be computed from Fourier series about either $\omega = i\infty$ or $\omega = 1$. Tables 3, 4 and 5 were constructed with expansions about $\omega = i\infty$. These series are accurate throughout much of R_0 and along most of sides 1, 3, 4 and 6. However, as ω approaches the real axis the Fourier series about $\omega = i\infty$ must diverge, which makes them unusable on sides 2 and 5 near $\omega = \pm 1$. However, just in these regions of R_0 where expansions about $i\infty$ converge slowly, we may use the alternative expansions about the cusp at $\omega = 1$ (equations (27*a*, 27*b*)) which will be most accurate near $\omega = \pm 1$. To illustrate this possibility we show in table 6, for a typical ρ value, the phase and modulus of $E(\omega, A_1)$ on sides 2 and 3 of R_0 evaluated by the alternative expansions. By using such Fourier series about all available parabolic cusps, one can cover the entire fundamental region R_0 to the same accuracy.

Table 6. Expansions for $E(\omega, A_0)$ ($\rho = \sqrt{3}$) about $i\infty$ and $+1$

$\omega = x+iy$			Expansion about $\omega = i\infty$		Expansion about $\omega = 1$	
x	y	Side	Modulus	Phase (rad)	Modulus	Phase (rad)
0·1	0·57	3	3·614	0·349	3·515	0·344
0·2	0·54	3	2·860	0·710	2·847	0·699
0·3	0·49	3	1·564	1·100	1·571	1·092
0·4	0·42	3	0·431	1·473	0·422	1·520
0·7	0·33	2	3·547	0·205	3·466	0·200
0·8	0·31	2	2·380	0·875	2·470	0·823

7. Representations of the amplitude $T(s)$

We have now obtained an explicit uniformization of the surface $\hat{\mathscr{R}}$ by using the theory of automorphic forms. The function $\tilde{\Omega}(\omega)$ above maps the half plane H one-to-one and conformally onto $\hat{\mathscr{R}}$ as a covering of the s plane. However, $\tilde{\Omega}(\omega)$ is not yet normalized in the most useful way. Let us define a univalent function $\Omega(\omega)$ taking the value zero at $\omega = \alpha$, the value 4 at $\omega = \beta$, and the value ∞ at $\omega = 1$.

$$\Omega(\omega) = 4\left(\frac{\tilde{\Omega}(\omega)-\tilde{\Omega}(\alpha)}{\tilde{\Omega}(\beta)-\tilde{\Omega}(\alpha)}\right). \tag{43}$$

As shown in the Appendix, $\tilde{\Omega}(\omega)$ and $\Omega(\omega)$ are each real along the boundary of R_0 so that $s = \Omega(\omega)$ gives the cut s plane of figure 6. The position of the left hand branchpoint, $s = 4-m_e^2$, corresponds to the value of $\Omega(\omega)$ at $\omega = i\infty$. Since $\tilde{\Omega}(i\infty) = 0$

$$m_e^2 = 4\left(\frac{\tilde{\Omega}(\beta)}{\tilde{\Omega}(\beta)-\tilde{\Omega}(\alpha)}\right) \tag{44}$$

showing the relation of m_e to the modulus ρ through $\tilde{\Omega}(\omega)$.

Since $\hat{\mathscr{R}}$ was a branched covering of $\mathscr{R}$, the surface of $T(s)$, we now wish to point out that $T(s)$ can be regarded as a function on $\hat{\mathscr{R}}$ and hence that ω can be used to represent $T(s)$. Now $\hat{\mathscr{R}}$ differed from $\mathscr{R}$ by having an $s = 0$ branchpoint in each sheet. We can regard $T(s)$ as a meromorphic function on $\hat{\mathscr{R}}$ subject to certain analytic constraint equations which just remove those $s = 0$ branchpoints which $T(s)$ ought not to possess. There should be no $s = 0$ branchpoint on the physical sheet of $T(s)$ nor on any sheet reached by continuation through the left hand cut alone. These sheets are just those corresponding to R_0 and its translates by powers of S. Hence, we may regard $T(s)$ as a function $T(\omega)$ on H (and therefore on $\hat{\mathscr{R}}$) subject to the constraint equations

$$T(S^q W S^{-q}\omega) = T(\omega) \qquad q = 0, \pm 1, \pm 2, \ldots \tag{45}$$

which ensure that $T(s)$ takes the same values on both sides of the cuts associated with the unwanted branchpoints.

If we now use an N/D decomposition of $T(s)$ we may obtain simple analytic representations of $T(s)$ on H incorporating the constraints (45). Thus in the usual manner $D(s)$ will be a function with no left hand cut but possessing the unitarity cut in the physical

sheet. The absence of the left hand cut in the physical sheet means that $D(\omega)$ obeys

$$D(S\omega) = D(\omega). \tag{46}$$

Since we must pass through the unitarity cut to reach other sheets of $D(s)$, the $s = 0$ branchpoint should indeed be present on all sheets of $D(s)$ except the physical sheet where we remove it by requiring

$$D(W\omega) = D(\omega). \tag{47}$$

We see that $D(\omega)$ is nearly automorphic on Γ. Equations (46) and (47) tell us that we can represent $D(\omega)$ in at least two different ways, exactly as one expands an automorphic form at parabolic or elliptic vertices (Lehner 1964). Thus from (46) we deduce that $D(\omega)$ has a Fourier expansion in $\exp(i\pi\omega)$ about $\omega = i\infty$ ($s = 4 - m_\pi^2$). Equation (47) tells us that about $\omega = \alpha$ ($s = 0$), $D(\omega)$ depends only on the variable

$$\tau = \left(\frac{1 + i\rho\omega}{\rho\omega + i}\right)^2. \tag{48}$$

Expansions in either variable may be used to represent $D(\omega)$ over different regions of H or $\hat{\mathscr{R}}$. From a given determination of $D(\omega)$, $N(\omega)$ follows from the discontinuity relation for $D(\omega)$ as

$$N(\omega) = \frac{i}{2}\left(\frac{\Omega(\omega) - 4}{\Omega(\omega)}\right)^{-1/2} (D(\omega) - D(V\omega)). \tag{49}$$

Thus we have different representations of $T(\omega)$ arising from those for $D(\omega)$.

8. Conclusions

We have demonstrated above how uniformizing mappings for simple Riemann surfaces can be easily constructed from automorphic forms which in turn can be computed numerically in a fairly straightforward way. The presence of logarithmic branchpoints (parabolic fixed points) made the Fourier expansions of the Poincare series the natural technique for numerical calculation. Indeed, the existence of parabolic cusps was an essential tool in keeping track of zeros of the forms concerned. In our relativistic model above, we simultaneously uniformized four branchpoints. The procedure we used would work efficiently for even more branchpoints. The practical limitation in this respect is that the number of moduli increases with the number of branchpoints, necessitating a search through a multidimensional space of moduli in order to test linear independence of the cusp forms used. When the number of moduli gets too large, the procedure becomes unwieldy and impractical. Our procedure above assumed that the branchpoint s_{p+1} in figure 7 was logarithmic. If this is not so, the cuts can be chosen differently and the procedure will go through with obvious modifications. We have given the mapping explicitly from ω to s, $s = \Omega(\omega)$. The inverse mapping $\omega = \Omega^{-1}(s)$ would be given in the usual way (Lehner 1964) by a quotient of two solutions of a second order differential equation in s with rational coefficients. In the potential theory model this is the hypergeometric equation. In the relativistic model it would be Heun's equation. In fact, the mapping from ω to s is the more useful one and it is the easier to compute.

When these mappings arise from scattering amplitudes, they will offer new ways to represent the analyticity of such amplitudes as was shown in § 7. This makes possible

simple approximations in ω valid over larger regions than are the corresponding approximations in terms of energy variables (Choudhary and Jones 1970, Choudhary 1971). From the point of view of approximations the most important function of the mappings above is to move nearby logarithmic singularities as far away as possible, namely these branchpoints end up explicitly on the boundary of the surface as parabolic vertices on the real axis of ω. At the same time algebraic branchpoints are unwound so that in ω it becomes a case of approximating a meromorphic function by a rational one.

Finally, the ω plane gives the clearest possible picture of the structure of the physical and unphysical sheets and of the relation of one sheet to another. We saw above in the numerical calculations that in fact sheets far from the physical sheet contributed very little (of order c^{-2m}) to the numerical evaluation of the functions concerned. Thus, in the ω plane we have even a quantitative measure of what is a 'nearby' or 'far away' sheet.

Acknowledgments

The authors wish to express their appreciation of the stimulating atmosphere provided by both staff and postgraduate students in this department. One of us (RBJ) wishes to acknowledge a most helpful conversation with Professor A M Macbeath of the Department of Mathematics, University of Birmingham. ARC would like to thank Queen Mary College for providing a Research Studentship.

Appendix

Here we wish to establish the identity

$$G_{-2m}(\omega, 1, A_j, \Gamma, v) = \overline{G_{-2m}(-\bar{\omega}, 1, A_j, \Gamma, v)} \tag{A.1}$$

for the generalized Poincare series of equation (24). Property (A.1) arises because the fundamental region R_0 of figure 8 was constructed to be symmetric under reflection in the imaginary ω axis. This property in turn followed from the real analyticity of the model amplitude $T(s)$. Thus, consider the transformation

$$R = \begin{pmatrix} \mathrm{i} & 0 \\ 0 & -\mathrm{i} \end{pmatrix}$$

which is involved in reflecting through the imaginary ω axis, $\omega \to -\bar{\omega} = \overline{R\omega}$. For a general transformation $M = \left(\begin{smallmatrix} a & b \\ c & d \end{smallmatrix}\right)$ we have

$$RMR^{-1} = \begin{pmatrix} a & -b \\ -\mathrm{c} & d \end{pmatrix}.$$

We first want to show that the set of matrices $A_j\Gamma$ is invariant under R, that is, for any M in $A_j\Gamma$, RMR^{-1} is also in $A_j\Gamma$. To do this note that

$$RA_j\Gamma R^{-1} = RA_jR^{-1}R\Gamma R^{-1}.$$

Also it is evident that

$$RA_0R^{-1} = A_0 \qquad RA_1R^{-1} = A_1S$$
$$RSR^{-1} = S^{-1} \qquad RWR^{-1} = W^{-1} \qquad RVR^{-1} = V^{-1}.$$

Remembering that Γ is generated by S, V, W, we see that $R\Gamma R^{-1} = \Gamma$ and hence

$$RA_j\Gamma R^{-1} = A_j\Gamma.$$

From (24) we have

$$G_{-2m}(\omega, 1, A_j, \Gamma, v) = \sum_{L\in(S)} (c\omega+d)^{-2m} \exp\left\{\frac{\mathrm{i}2\pi v}{\lambda_j}\left(\frac{a\omega+b}{c\omega+d}\right)\right\}$$

where $L = \left(\begin{smallmatrix} a & b \\ c & d \end{smallmatrix}\right)$ and we sum over all distinct L in $A_j\Gamma$ with different second row. Obviously

$$G_{-2m}(-\bar{\omega}, 1, A_j, \Gamma, v) = \sum_{L\in(S)} (-c\bar{\omega}+d)^{-2m} \exp\left\{\frac{-\mathrm{i}2\pi v}{\lambda_j}\left(\frac{a\bar{\omega}-b}{-c\bar{\omega}+d}\right)\right\}.$$

But to each matrix $\left(\begin{smallmatrix} a & b \\ c & d \end{smallmatrix}\right)$ corresponds another $\left(\begin{smallmatrix} a & -b \\ -c & d \end{smallmatrix}\right)$, hence

$$G_{-2m}(-\bar{\omega}, 1, A_j, \Gamma, v) = \sum_{L\in(S)} (c\bar{\omega}+d)^{-2m} \exp\left\{\frac{-\mathrm{i}2\pi v}{\lambda_j}\left(\frac{a\bar{\omega}+b}{c\bar{\omega}+d}\right)\right\}$$

$$= \overline{G_{-2m}(\omega, 1, A_j, \Gamma, v)}.$$

From (A.1) and (11) follows immediately a knowledge of the phase of these functions on the boundary of R_0 and on the imaginary axis. Consider $E(\omega, A_0)$ as an example. On the imaginary axis $\omega = \mathrm{i}|\omega|$, equation (A.1) gives

$$E(\mathrm{i}|\omega|, A_0) = \overline{E(-\mathrm{i}|\omega|, A_0)} = \overline{E(\mathrm{i}|\omega|, A_0)} \tag{A.2}$$

that is, $E(\omega, A_0)$ is real there. Next let ω lie on side 6 of R_0. By (11), $E(S\omega, A_0) = E(\omega, A_0)$, but, for ω on side 6, $S\omega$ is on side 1 and $S\omega = -\bar{\omega}$ giving

$$E(S\omega, A_0) = E(-\bar{\omega}, A_0) = E(\omega, A_0).$$

Using (A.1) we get

$$E(\omega, A_0) = \overline{E(\omega, A_0)} \tag{A.3}$$

for ω on side 6. Thus $E(\omega, A_0)$ is real on sides 6 and 1. Next let ω lie on side 2. Then $V\omega$ is on side 5 and $V\omega = -\bar{\omega}$. Hence by (11) $E(V\omega, A_0) = \{-(\gamma+1)\omega+\gamma\}^4 E(\omega, A_0)$, and $E(V\omega, A_0) = E(-\bar{\omega}, A_0) = \overline{E(\omega, A_0)}$ by (A.1). Thus for ω on side 2

$$\frac{E(\omega, A_0)}{\overline{E(\omega, A_0)}} = \{-(\gamma+1)\omega+\gamma\}^{-4}.$$

Now $|-(\gamma+1)\omega+\gamma| = 1$ is the equation of the circle of which side 2 is an arc. Thus the phase of $E(\omega, A_0)$ satisfies

$$\arg E(\omega, A_0) = -2\arg\{-(\gamma+1)\omega+\gamma\} + n\pi \tag{A.4}$$

for ω on side 2. Similarly, for ω on side 5

$$\arg E(\omega, A_0) = -2\arg\{(\gamma+1)\omega+\gamma\} + n\pi \tag{A.5}$$

while for ω on sides 3 or 4

$$\arg E(\omega, A_0) = -2\arg(\rho\omega) + n\pi. \tag{A.6}$$

As a consequence of these exact phase relations, $\tilde{\Omega}(\omega)$ and $\Omega(\omega)$ are real everywhere on the boundary of R_0 and also on the imaginary ω axis.

References

Baluny V Z 1969 *Institute for Theoretical Physics Kiev Preprint* 69–15
Choudhary A R 1971 *PhD Thesis* University of London pp 118–37
Choudhary A R and Jones R B 1970 *Nucl. Phys.* B **22** 343–57
Cutkosky R E and Deo B B 1968 *Phys. Rev.* **174** 1859–66
Ford L R 1951 *Automorphic Functions* (New York: Chelsea)
Frazer W R 1961 *Phys. Rev.* **123** 2180–2
Fricke R and Klein F 1897 *Vorlesungen uber die Theorie der automorphen Functionen* vol 1 (Leipzig: Teubner)
—— 1912 *Vorlesungen uber die Theorie der automorphen Functionen* vol 2 (Leipzig and Berlin: Teubner)
Jones R B 1970 *Commun. math. Phys.* **17** 143–55
Lehner J 1964 *Mathematical Surveys. Number* 8 (Rhode Island: American Mathematical Society)
Springer G 1957 *Introduction to Riemann Surfaces* (Reading, Massachusetts: Addison-Wesley)
Wanders G and Piguet O 1968 *Nuovo Cim.* A **56** 417–36